Poly(phenylacetylene) Derivatives for Nonlinear Optics

J. Le Moigne,* A. Hilberer, and C. Strazielle

Institut de Physique et Chimie des Matériaux de Strasbourg, Groupe des Matériaux Organiques, and Institut C. Sadron, 6 Rue Boussingault, 67083 Strasbourg, France

Received February 18, 1992;
Revised Manuscript Received August 5, 1992

Introduction

Recently very high optical nonlinear susceptibilities have been given in the literature on organic polymers: a third-order susceptibility, $\chi^{(3)}$, observed on a Shirakawa polyacetylene, $(CH)_x$, was about 10^{-9} esu,[1] and on an oriented $(CH)_x$ prepared by the Durham method, $\chi^{(3)}$ reached a value of 2.7×10^{-8} esu,[2] the highest value ever reported for an organic material. As compared, the third-order susceptibility measured along the chain in a polydiacetylene crystal is 8×10^{-10} esu.[3] These exceptionally high values of the electronic third-order susceptibility have led to the search for new derivatives with the same alternance in the conjugated chain as soluble polyacetylenes (PA), which can be conveniently processed using a casting method.

While the unsubstituted PA backbone in the all-trans $(CH)_x$ is perfectly planar and the electron delocalization occurs in the whole macromolecule, the backbone of a substituted PA can be planar or nonplanar depending on the side chain steric hindrance.[4] Moreover, $(CH)_x$ is extremely sensitive to doping and degradation, by oxidation of the double bonds of the polymer backbone; the doping reduces the transparency in the optical bandgap of the polymer (1.54 eV for pure trans $(CH)_x$).[5] Those effects can be lowered by the presence of side chains on the polyacetylenic backbone.

In a previous work[6] we presented for the first time the synthesis and the mesogenic properties of a soluble polyacetylenic derivative with a bulky cholesteryl group at the end of a flexible spacer. We reported the thermotropic liquid crystalline properties of the side chains, a smectic phase, joined to the hyperpolarizability properties of a polymer with a conjugated backbone. The moderated value of $\chi^{(3)} = 10^{-13}$ esu is consistent with the large molecular weight of the inactive side group and also with a moderate conjugation length of the PA chain. Moreover, a loss of conjugation takes place in solution or in the liquid phase, which we presently attribute to the lowering of the interaction strains between the side chain methylene and the ethylenic proton of the PA chain.

In this work we present the synthesis, the characterization, and the properties of a series of poly(phenylacetylene) derivatives which are compared to the cholesterylpolyacetylene. We expected that the lateral phenyl rings could be arranged in stacks, and that this organization along the backbone could preclude the torsional motions around the single bonds of the chain.

Experimental Section

We have synthesized a series of 4-ethynylbenzoates (methyl to hexadecyl and phenyl benzoates), which were then polymerized using the classical WCl_6 catalyst.

Materials and Synthetic Methods. The 4-bromobenzoic acid, linear alcohols, dicyclohexylcarbodiimide (DCCI), (dimethylamino)pyridine (DMAP), methylene chloride (CH_2Cl_2) (HPLC grade), (trimethylsilyl)acetylene (TMSA), palladium(II) acetate ($Pd^{II}Ac_2$), triphenylphosphine (PPh_3), tetrabutylammonium fluoride (TBAF) (1.1 M in THF), and tungsten hexachloride (WCl_6) were obtained from Aldrich, and used without further purification. Triethylamine (Aldrich) was distilled from KOH before use. Toluene and 1,4-dioxane were distilled from Na and kept under vacuum.

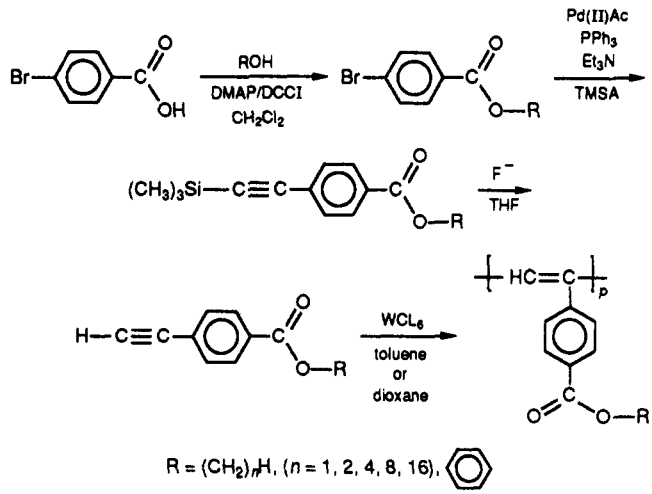

A typical example of synthesis is given hereafter for the C16 derivative.

Preparation of Hexadecyl 4-Bromobenzoate (I). To an ice-cooled and stirred solution of 4-bromobenzoic acid (5.43 g, 27.0 mmol), 1-hexadecanol (6.60 g, 27.2 mmol), and DMAP (0.227 g, 1.9 mmol) in 150 mL of CH_2Cl_2 was added dropwise the DCCI (5.76 g, 27.9 mmol) dissolved in 5 mL of CH_2Cl_2. The mixture was then stirred at room temperature for 24 h. The formed urea was filtered off and the solution evaporated under vacuum. The crude product was passed through a silica gel column, eluent CH_2Cl_2–heptane (50:50), to give 11.0 g (25.8 mmol) of ester. Yield: 95%. ^1H NMR: δ 8–7.5 (4 H, ArH), 4.28 (2 H, t, OCH_2), 1.75 (2 H, q, OCH_2CH_2), 1.6–1.1 (26 H, 13 CH_2), 0.87 (3 H, t, CH_3).

Preparation of Hexadecyl 4-[(Trimethylsilyl)acetenyl]benzoate (II). To a solution of hexadecyl 4-bromobenzoate (11.0 g, 25.8 mmol) in 150 mL of triethylamine under nitrogen were added $Pd^{II}Ac$ (0.055 g, 0.25 mmol), PPh_3 (0.134–0.51 mmol), and finally TMSA (5.5 mL, 39 mmol). The mixture was heated at 70 °C and stirred under nitrogen for 24 h. After cooling the precipitated salt was filtered and the solvent evaporated. The product was dissolved in 50 mL of CH_2Cl_2 and the solution washed twice with 50 mL of a 0.5 N HCl solution. The organic phase was dried over Na_2SO_4 and evaporated. The crude brown product was purified on a silica gel column using CH_2Cl_2–heptane (50:50) as solvent, to give 10.31 g (23.3 mmol) of silylated acetylenic ester. Yield: 90%. ^1H NMR: the same as that for I and δ 0.27 (9 H, s, $(CH_3)_3Si$).

Preparation of Hexadecyl 4-Ethynylbenzoate (III). Hexadecyl 4-[(trimethylsilyl)acetenyl]benzoate (10.3 g, 23.3 mmol) was dissolved in 150 mL of THF. TBAF (2 mL, 2.2 mmol) was added slowly, leading to a black solution. The reaction was stopped by filtering the solution on silica gel. After THF evaporation, the black product was passed through a silica gel column with eluent CH_3CCl_3, giving a yellow product which was recrystallized from CH_2Cl_2–pentane to give 2.90 g (7.8 mmol) of hexadecyl 4-ethynylbenzoate. Yield: 34%. ^1H NMR: the same as that for I and δ 3.23 (1 H, s, CCH). IR: 3300 (≡C—H), 2110 (C≡C), 1720 cm^{-1} (C=O). Anal. Calcd: C, 81.03; H, 10.34. Found: C, 80.90; H, 10.55. Mp: 48 °C.

Preparation of Poly(hexadecyl 4-ethynylbenzoate) (IV). The polymer was prepared according to the previously reported procedure,[6,7] using the WCl_6–toluene system. Polymer yield: 70%; IR: no acetylenic bands at 3300 and 2110 cm^{-1}. Anal. Calcd: C, 81.03; H, 10.34. Found: C, 80.53; H, 10.67.

Instruments and Methods. Polymer molecular weights were obtained by size exclusion chromatography (SEC) in eluent THF with the coupled detection of refractive index and light scattering on a previously described apparatus.[8] Infrared spectra of thin solid films deposited on KBr plates were recorded on a Perkin-

0024-9297/92/2225-6705$03.00/0

Table I
SEC Results on PPA Derivatives of Different Lengths of the Alkyl Ester Chain or Phenyl Substituent[a]

PPA derivative	$\langle M_w^{LS} \rangle$	$\langle M_w^{SEC} \rangle$	$I = \langle M_w \rangle / \langle M_n \rangle$
PPAC1	71 400	39 700	2.52
PPAC2	79 200	47 000	2.75
PPAC4	78 300	46 000	1.79
PPAC8	55 700	31 700	2.82
PPAC16	131 000	79 300	1.60
PPAPh	109 000	51 000	1.71

[a] $\langle M_w^{LS} \rangle$ represents the weight-average molecular weight from coupled results of SEC and light scattering on line; $\langle M_w^{SEC} \rangle$ represents the apparent weight-average molecular weight from the polystyrene calibration (PS equivalent); I is the heterogeneity index (measured by SEC).

Table II
Comparison between the Intrinsic Third-Order Susceptibilities, $\chi^{(3)*}$, Calculated for a Perfectly Oriented Polyacetylenic Chain, from Different Literature Results and from This Work

PA chain	$\chi^{(3)*}$ (esu) (calcd for oriented PA chain)	ref
$(CH)_x$ (t) (Durham)	2.7×10^{-8} [a]	2
$(CH)_x$ (t) (Shirakawa)	4.2×10^{-9}	9
PPA	2.8×10^{-11}	11, 22
o-TSPPA	1.6×10^{-10}	11, 22
*p*CP5	9×10^{-12}	6
$PPAC_1$	1.6×10^{-11}	this work

[a] Experimental value.

Elmer 983 infrared spectrophotometer. Ultraviolet absorption spectra were measured in THF or in cast solid films on quartz substrates, with a Shimadzu UV-2101PC UV–vis scanning spectrophotometer. Differential scanning calorimetry (DSC) was performed on a Perkin-Elmer DSC7. Melting points were determined on an electrothermal digital melting point apparatus or by DSC. Thermogravimetric analyses were realized with a Mettler TA3000 system.

^1H and ^{13}C NMR spectra were obtained in $CDCl_3$ with Brüker AC-200F spectrometer at room temperature or with a variable-temperature probe. The resonance raman (RR) scattering was performed on thin solid films at the excitation wavelengths of an argon–neon laser at 457.9 and 514.5 nm. The scattered intensities were recorded through a double monochromator with a spectral slit width of 5 cm^{-1}.

The nonlinear optical characterization was carried out by third harmonic generation measurements (THG) on solid thin films prepared by casting or dipping. The experimental details have been previously described.[9]

The molecular modeling was performed with Sybyl software from Tripos, running on a DEC Vax unit linked with a graphic unit from Evans and Sutherland.

Results

We prepared a series of alkyl or aryl esters of poly(phenylacetylene) (hereafter abbreviated PPACn or PPAPh) by the methods already described in the literature and also precisely defined in a previous paper on polyacetylenic derivatives.[10] The polymerization is characterized by a better yield (75%) in toluene than in dioxane (50%); all polymers of the series are perfectly soluble in common solvents (toluene, THF, chlorocarbons, etc.). Thin transparent films of blood red color can be made by dipping, casting, or spin coating from solution.

Characterization of Polymer in Solution. The molecular weight analysis by SEC was coupled with "on-line" refractive index and light scattering detection. In Table I we give $\langle M_w^{SEC} \rangle$, the weight-average molecular weight deduced from the polystyrene (PS) standardization of the column, and $\langle M_w^{LS} \rangle$, a direct determination of the weight-average molecular weight obtained from the light scattering measurements. In Figure 1a we have plotted the light scattering molecular weight (M_w^{LS}) vs the elution volume of the column for PPAC4, PPAC16, PPAPh, and standard polystyrene. By using the principle of universal calibration, $[\eta]$, the intrinsic viscosity of a polymer fraction at the elution volume V_e can be calculated from the following relations:

$$[\eta]^{PS} M_w^{SEC} = [\eta] M_w^{LS}$$

$$[\eta] = [\eta]^{PS} M_w^{SEC} / M_w^{LS}$$

where $[\eta]^{PS}$ is the intrinsic viscosity of PS corresponding to the molecular weight M_w^{SEC}. In this determination of the molecular weight we expected that the chromatographic separation proceeds only by a size exclusion mechanism, without any absorption of the polymer on the column. Figure 1b represents the curves log $[\eta] = f(\log M_w)$, which are established here for the same polymers as in Figure 1a. Points at the two extremes of the scale are subject to considerable experimental error and were therefore ignored. The plots obey the Mark–Houwink equation $[\eta] = KM^{\alpha}$. The two coefficients K and α are not significantly different for the different side chain lengths n of the series. Thus, we have represented an average fit, where $K = 4.27 \times 10^{-4}$ and $\alpha = 0.92$, taking in account all the PPACn polymers. The exponent α, larger than those of usual saturated chains (i.e., for standard polystyrene $\alpha = 0.70$ in THF), proves that the polymers in solution are in an extended conformation. The curve of the phenyl derivative leads to slightly different parameters: $K = 1.6 \times 10^{-4}$ and $\alpha = 0.97$. The straight line is quite parallel to the others; for the same molecular weight, the intrinsic viscosity is lower than those of the alkyl derivative.

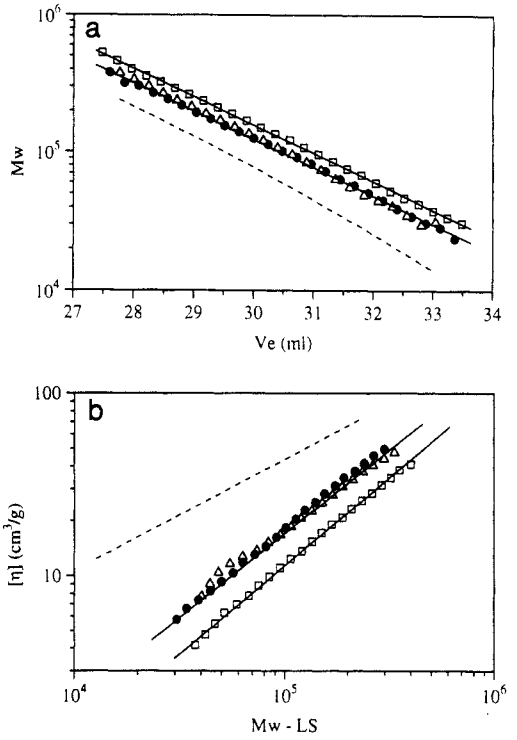

Figure 1. Size exclusion chromatography (SEC) characterization of PPA polymers in THF (●, PPAC4; ▲, PPAC16; □, PPAPh; dashed line, PS): (a) molecular weight vs elution volume; (b) intrinsic viscosity of the polymer vs molecular weight.

Optical Properties. The absorption spectrum of a polymer solution of PPAC16 is represented in Figure 2. The UV–vis spectrum is the same for the solution and for a solvent-cast film. A similar effect was recently reported for other poly(phenylacetylene) derivatives.[11] Only ul-

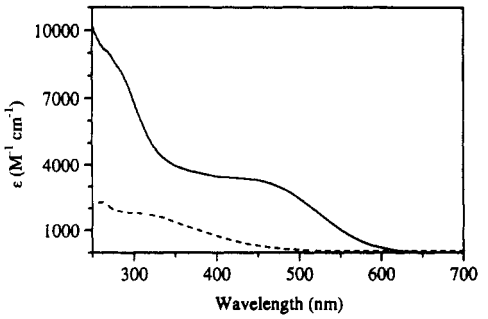

Figure 2. Electronic absorption spectra in THF: molar absorption coefficient vs wavelength for PPAC16 (continuous line) and PCP5 (dashed line).

trathin spin-coated films showed distinct differences in their spectra, and these were attributed to a preferred orientation of polymer chain parallel to the substrate. The absorption spectrum of Figure 2 shows a large absorption band with a cutoff at about 600 nm and a large shoulder at 450 nm. This absorption band is red-shifted as compared with the spectrum of the PA cholesteryl derivative where the shoulder in solution was at about 325 nm (dotted line in Figure 2). This increase in the conjugation length of the PA backbone is a result of the polymerization of the PPA derivative.

Nonlinear measurements were carried out on solid films of PPAC16 and PPAC1 prepared by casting. The third-order susceptibilities were investigated by third harmonic generation ($\chi^{(3)}(-3\omega;\omega,\omega,\omega)$), and the measurements were performed at incident wavelength of 1.9 μm. Thus, $\chi^{(3)}(-3\omega;\omega,\omega,\omega)$ is far from resonances at two or three photons for poly(phenylacetylenes),[12] and the $\chi^{(3)}$ determinations are purely real. The magnitudes of $\chi^{(3)}$ are 6×10^{-13} esu for PPAC16 and 8×10^{-13} esu for PPAC1. These values are greater than the values in the PA cholesteryl derivative by a factor of 6, and they show that the red shift of the linear absorption band can be correlated to an enhancement of the third-order susceptibility. A complete discussion of properties relating to the unsaturated backbone is given further on in this note.

Characterization of the Polymer Backbone: Raman and ^{13}C NMR Spectroscopies. Resonance Raman spectroscopy was carried out on thin solid films of PA with cholesteryl side chains and on PPA derivatives with aliphatic side chains. The scattered Raman spectra were collected from the excitation of the long wavelength part of the π–π^* electronic transition in the conjugated polymeric system. The excitation laser wavelengths were 514.5 and 457.9 nm for the PCP5 and 514.5 nm for PPAC16. The Raman data of the two polymers are plotted in Figure 3. The spectra are dominated by the two resonance groups of the C=C double bond stretching appearing between 1600 and 1500 cm^{-1} and the C—C single bond stretching in the range of 1300–1100 cm^{-1}.[13a] A single peak is observed at 1175 cm^{-1} for the PCP5 and 1225 cm^{-1} for the PPAC16 corresponding to the C—C bond. The other part of the spectra around 1500 cm^{-1} is very interesting: a single peak is observed at 1525 cm^{-1} on the PCP5 spectrum, and twin peaks are observed at 1525 and 1499 cm^{-1} for the poly(phenylacetylene) derivative. The resonance at 1525 cm^{-1} is characteristic of the stretching of the cis double bond, and the resonance at 1499 cm^{-1} is characteristic of the stretch of the trans C=C.[13b] The polymer backbones are strongly different, and the attempt to analyze the backbone conformations could be realized by NMR analysis.

Figure 4a shows the ^{13}C NMR spectrum of the PPAC1 obtained with WCl_6 in dioxane. The spectrum is well resolved as for all polymers of the series prepared in

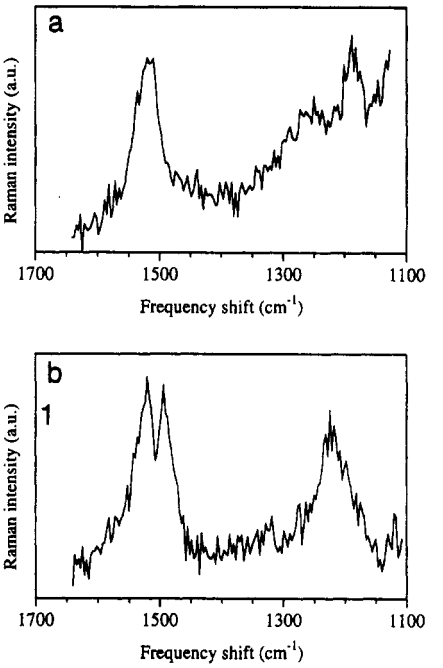

Figure 3. Raman resonance spectra of acetylenic bonds: (a) PCP5 spectrum; (b) PPAC16 spectrum.

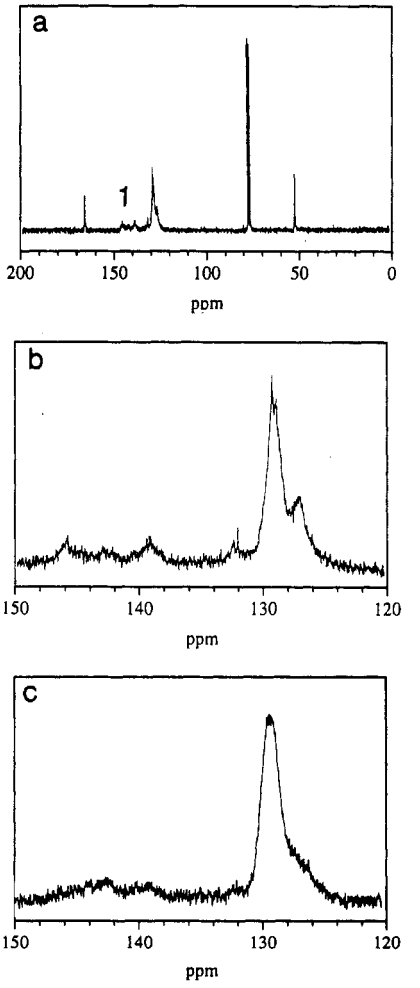

Figure 4. ^{13}C NMR spectra of PPAC*n* in $CDCl_3$: (a) spectrum of PPAC1 (polymerization with WCl_6/dioxane); (b) unsaturated carbon region of PPAC1 (WCl_6/dioxane) spectrum; (c) unsaturated carbon region of PPAC1 (WCl_6/toluene) spectrum.

dioxane. For the attribution all resonances can be separated in three ranges, the 170–160 ppm range attributed to the carbonyl carbon atom, the 150–120 ppm range attributed to the unsaturated carbon atoms, and the 70–

10 ppm range attributed to the saturated carbon atoms. The unsaturated carbon range is particularly interesting, and an expansion of these regions is presented in Figure 4b,c for the same polymer (PPAC1), prepared in two different solvents (dioxane and toluene) with the same catalyst (WCl_6). Six peaks can be clearly observed in Figure 4b. As identified by Percec et al.[14] for the microstructure of poly(phenylacetylene), the resonances between 120 and 132 ppm are assigned to the tertiary carbons, whereas the resonances between 135 and 147 ppm are assigned to the quaternary carbons. Following Percec, the intense peak at 129.4 ppm is attributed to the phenyl carbons 2–6, the peak at 127.0 ppm is attributed to the carbon β in the trans conformation (βt), and the resonance at 132.0 ppm is assigned to the carbon β in a cis conformation (βc).

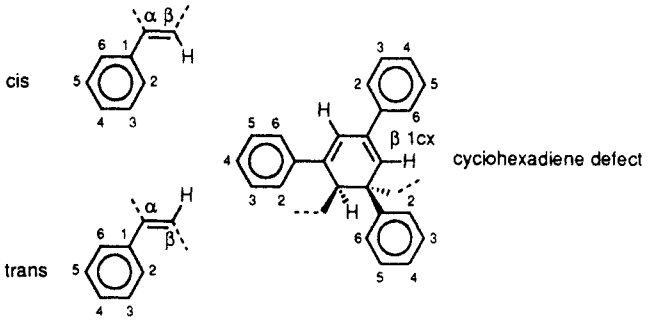

The peaks of the quaternary carbons are much less intense. The signals at δ 142.8–143.0 and 139.3 ppm are identified as Cα (cis and trans) and C1 (cis and trans) of the aryl group, respectively. The third resonance at δ 146.1 ppm has been identified by Percec et al.[14] as quaternary carbons in cyclohexadiene sequences. Other characteristic signals of these sequences at δ 129.3 ppm (noted as β1cx) should be partially masked by Cβ trans or the aryl carbons C2–6. Figure 4c shows a much less resolved spectrum for PPAC1 polymerized in toluene. First the Cβ trans resonance appears as a shoulder of the intense peak centered at 129.1 ppm, indicating a lower content in trans sequences. In the spectrum, the quaternary carbon part, also poorly resolved, confirms, by a large peak at 142.5 ppm, a distribution of cis–trans conformations, and no signal at 146.1 ppm shows that the polymer contains a lower concentration of hexadiene defects than the previous one.

Thermal Properties. Thermogravimetric analysis (TGA) reveals the considerable thermal stability of all of the compounds in the PPAC*n* series, in both air and nitrogen atmospheres up to 330 °C (Figure 5a).

The differential scanning calorimetry (DSC) of short side chain poly(phenylacetylene)s (*n* from 1 to 4 carbon atoms) shows no enthalpic or T_g transitions. For long side chains the DSC curve shows a single peak, indicating a single enthalpic transition. For PPAC8 a broad peak is centered at 75 °C, and the enthalpic transition gives ΔH = 4.4 kJ/mol, whereas for PPAC16 the transition temperature decreases to 26 °C and the enthalpy increases to ΔH = 14.8 kJ/mol. These values are consistent with a semicrystalline structure, but no glass transition is seen. From lowering of the transition temperature, passing from C8 to C16, we concluded that the enthalpic transition is due to the melting of side chains. Moreover, we attributed the lack of a glass transition temperature in the experimental range to the relative stiffness of the main chain[15a] and to the immobility of the ethylenic segments in the backbone.

For the PPAC16 the enthalpic properties depend strongly on the thermal history of the sample: during the first heating a single peak is observed at 11 °C, which is shifted to 26 °C in the following heatings (Figure 5b). A treatment at room temperature for several hours induces new thermal transitions after the main peak.

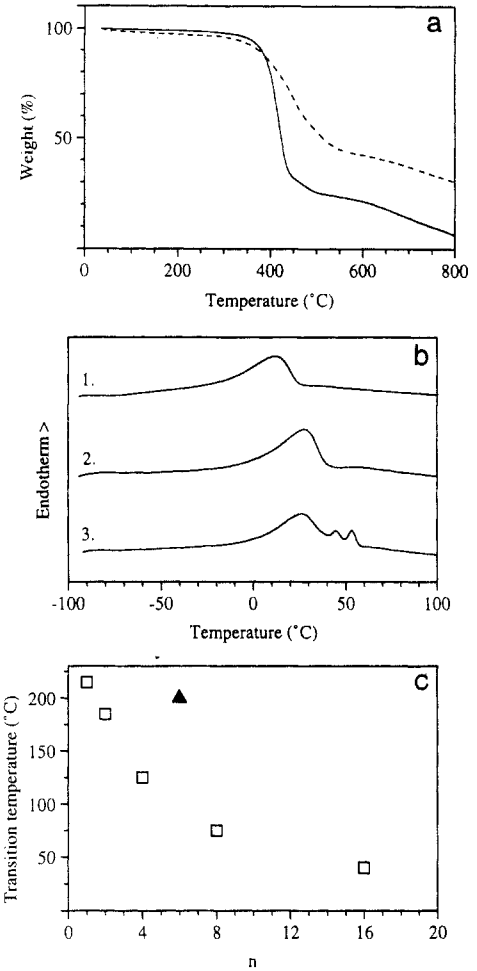

Figure 5. Thermal analysis of PPA esters: (a) TGA curve of PPAC1 (dotted line) and PPAC16 (continuous line); (b) DSC thermogram of the PPAC16 derivative at 10 °C/min (curve 1, first heating; curve 2, second heating; curve 3, heating after 24 h at room temperature); (c) melting points of PPAC*n* versus *n* and PPAPh.

Optical microscopy of the thin films showed no liquid-crystalline (LC) phase in any temperature range, for any polymer in the series; however, a melting transition of the polymers was observed with an increase of the temperature. These "melting points" are given in Figure 5c. For long side chains (C8 and C16) these transitions are superimposed on the enthalpic transitions observed by DSC.

The X-ray diffraction patterns of the PPAC8, recorded at 120 °C, show a rather broad diffraction ring in the small angle region, and a diffuse band in the wide angle region. The average spacing corresponding to the small angle reflection is 24 Å. At this time we are not able to correlate this periodicity to a specific mesomorphic structure. The diffraction bands disappear above 160 °C.

We conclude that the thermal studies of this series of poly(phenylacetylene) derivatives show amorphous or semicrystalline properties, for short or long side chains, respectively, and the lack of glass transition could be related to the high backbone stiffness.

Discussion

The effects of local rigidity changes on the conformation of very simple saturated polymers in good solvents were shown by Aime and co-workers:[16] the origin of the local

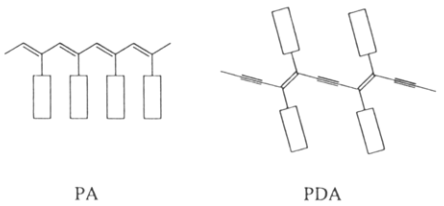

Figure 6. Schematic difference in the geometries of planar polyacetylene (PA) and polydiacetylene (PDA) with side chains.

rigidity can be related to the extension of the side groups and the average rotation between monomer units. The variation of the statistical length as a function of the lateral extension suggests the same type of behavior for both conjugated and saturated polymers. The conjugation along the backbone will have a relatively small influence on the local stiffness as compared to the size effect of the substituent (increase of the stiffness with increase of the length of the side chain). In their work they related the conjugation length to the torsion of the chain, and it has been expected that the same behavior will be observed in the conjugated backbones of the polydiacetylenes and of the substituted polyacetylenes.

However, there are some differences between the two types of polymers: firstly, the rotation around a single bond in a PDA can be considered as free (2.5 kJ/mol, about kT[16]), while the rotation around a single bond in a PA is not free (5.8 kJ/mol[17]); secondly, the backbone of a substituted PA is more crowded than those of a substituted PDA. The repetitive units have the length of two carbons in the PA backbone, and four carbons in the PDA (Figure 6). Therefore, the PDA derivatives should be more flexible in solution than the PA derivatives.

In the PPAC*n* and PPAPh derivatives we obtain a relatively high power in the Mark–Houwink equation (α = 0.92), a value which characterizes a more rigid backbone than for cholesterylpolyacetylene (α = 0.67). Other high values of α were also observed in some crowded PA such as the poly(chloroalkynes) or poly[1-(trimethylsilyl)-1-propyne], where α extends between 0.9 and 1.1.[4,18] The low α measured for some fluorine PPA derivative[19] (α = 0.60 in the [*o*-(trifluoromethyl)phenyl]acetylene) could be related to solvent and temperature effects.[15b] An interesting point in our work is that the α value is almost independent of the side chain length and of the substituent nature (alkyl or phenyl). This means that the high value of α, characteristic of the chain stiffness, is mainly due to the phenyl ring directly attached to the backbone. The influence of the alkyl chains or of the second ring is very low.

The conformations of the polyacetylenic chain, characterized by Raman resonance and NMR spectroscopies, lead to a mixing of cis and trans chain microstructures. The ^{13}C NMR resonance bands of the unsaturated carbon atoms of PPAC*n* are broaded by reference to the ^{13}C NMR spectra of the "stereoregular PPA" of Furlani et al., polymerized with Rh(I) catalysts.[20] They conclude an all head to tail regular structure, whereas we suggest that the PPAC*n* present a much more complex microstructure.

The modelization of PPA chains can visualize the different planar structures, which might be formed during the polymerization. Figure 7 represents PPAC8 in different planar trans and cis configurations. The trans addition of monomers in head to tail or head to head positions (see Figure 7) leads to distances between phenyl groups, respectively, of 2.4 and 4.8 Å. The head to tail addition is unlikely because the distance between two phenyl rings of 2.4 Å is too short to respect the van der

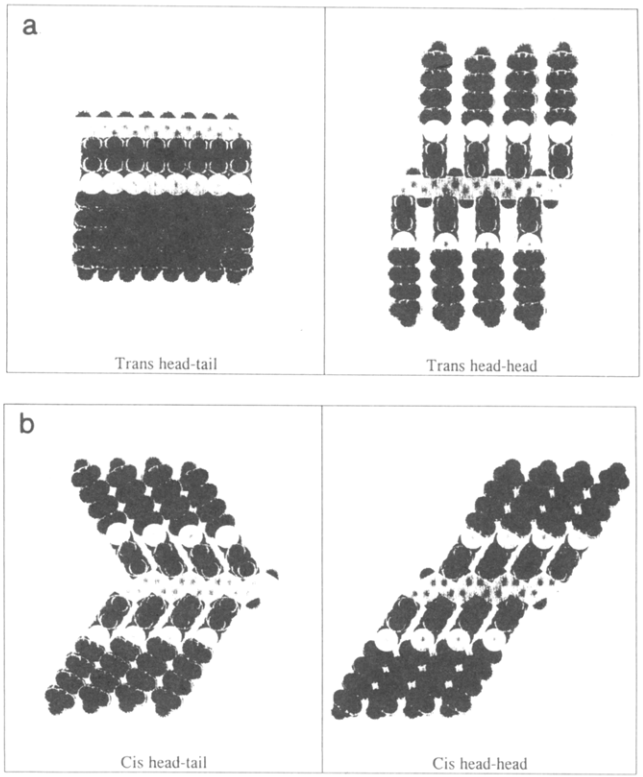

Figure 7. Computer models of planar polymer backbones obtained by head to head and head to tail additions: (a) trans head to tail and trans head to head; (b) cis head to head and cis head to tail.

Waals volume of phenyl substituents arranged in stacks. The head to head addition, where the side chains are organized in a double layer along the main chain, gives also a place in the 4.8 Å between the phenyl groups and the single H of the PA chain. This polymerization addition is the most favorable planar configuration. The cis head to tail and head to head addition of monomer gives a herringbone arrangement of side chains. The distance between phenyl rings is about 3.8 Å for the two configurations, a distance where the van der Waals interactions between phenyl rings remain low and the crystallization of alkyl chains will be possible. During the polymerization the planar metal complex, which is a key intermediate in the propagation reaction, can be expected to be very crowded sterically during the assembly of cis or trans dyads.[21a,b] The crowding of the planar carbene could explain the formation of the head to head planar configuration of the PA backbone.[21c]

We noted that the $\chi^{(3)}$ of the cholesterylpolyacetylene is around 10^{-13} esu; it decreased with the lowering of the conjugation length due to relaxation of the steric interactions between the ethylenic proton and the side group. The relaxation of strains by motions in the polymer chain is highly enhanced in good solvents or in the melt. In PPAC*n* the values of $\chi^{(3)}$ are 7 or 8 times higher than in cholesterylpolyacetylene. The intrinsic third-order susceptibilities of the PA backbone, $\chi^{(3)*}$, are given in Table II for polymers of this work or other PA from the literature.[2,5,11,22] All values were calculated relating to a PA chain where the contribution of the side chain to the molecular hyperpolarizability is negligible. Assuming that polyacetylene samples were perfectly isotropic, we calculated $\chi^{(3)*}$ for a hypothetically oriented chain by using a corrected factor of $1/\langle\cos^6\theta\rangle = 16/5$.[2] The disparity between all the $\chi^{(3)*}$ values becomes very large: the first difference between $(CH)_x$ can be explained as a difference

in packing density of the solid,[2] while the $\chi^{(3)}$* of the substituted PA are significantly lower. $\chi^{(3)}$* of simple PPA is 3 orders of magnitude lower than that of the Durham polymer; the better result for a substituted PA is obtained in poly[*o*-trimethylsilyl)phenylacetylene], *o*TSPPA, where $\chi^{(3)}$* is 2 orders of magnitude lower than that of the $(CH)_x$ reference. We obtained, for PPAC*n*, a $\chi^{(3)}$* of the same value as that for PPA from ref 16. These results are consistent with the observation of a red shift in the spectral absorption of *o*TSPPA (λ(max) = 550 nm) related to PPAC1 (shoulder at 450 nm) and PPA (shoulder at 430–450 nm). The values of the electronic absorption bands of the polymers in solution are also consistent with large differences in $\chi^{(3)}$*. The two absorption curves of PPAC1 and PCP5 with the same molecular absorption scale are strongly different as represented in Figure 2.

Such properties of the polymer chain lead to the notion of a "planar fraction" or "defect fraction" in the PA backbone. We suggest that in a conjugated polymer two kinds of defects take place in the backbone: firstly, conformation defects such as helicoidal segments caused by the cis cisoidal conformation of =C—C= bonds and, secondly, chemical defects such as quaternary saturated carbons. All these defects interrupt the electron delocalization; thus, the length of conjugation is reduced and the concentration of hyperpolarizable segments decreases.

Conclusion

The alkyl and phenyl ester derivatives of poly(phenylacetylene) are largely soluble in common solvents and present high molecular weights. The $\chi^{(3)}$ values of PPAC*n* are 7–8 times higher than those of previously prepared polyacetylenic derivatives with flexible substituents. This result is in agreement with the spectroscopic optical properties, i.e., a red shift of the absorption band and a high molar absorption with respect to poly(cholesterylacetylene). Nevertheless, the $\chi^{(3)}$ reported for the whole polyacetylenic chain is 3 orders of magnitude lower than $\chi^{(3)}$ of the $(CH)_x$ polymer and lower than $\chi^{(3)}$ values given in the literature for some substituted derivatives. The molecular modeling shows that the most probable planar configuration is the trans head to head alternance, which gives the best van der Waals distance between the lateral substituents. We attribute the low value of the third-order susceptibility to the presence of nonplanar forms (helicoidal cis cisoidal form, etc.) and chemical defects, such as cyclohexadiene cyclizations, which take place in the polyacetylene backbone. Improvements in the conjugation length and in $\chi^{(3)}$ of side chain poly(phenylacetylene) may be obtained not only by lowering the chemical defects but also by an increase of the content in the planar trans head to head configuration.

Acknowledgment. The authors are grateful to Dr. F. Kajzar for the nonlinear optical measurements and Dr. J. C. Merle for Raman measurements. We also thank Dr. K. Matyjaszewski for his fruitful suggestions.

References and Notes

(1) Kajzar, F.; Etemad, S.; Baker, G. L.; Messier, J. *Solid State Commun.* **1987**, *63*, 1113.
(2) Drury, M. R. *Solid State Commun.* **1988**, *68*, 417.
(3) Sauteret, C.; Hermann, J. P.; Frey, R.; Pradère, F.; Ducuing, J.; Baughman, R.; Chance, R. R. *Phys. Rev. Lett.* **1976**, *36*, 956.
(4) Masuda, T.; Yoshimura, T.; Tamura, K.; Higashimura, T. *Macromolecules* **1987**, *20*, 1734.
(5) (a) Krautz, F.; Wintner, E.; Leising, G. *Opt. Rev. B* **1989**, *39*, 3701. (b) Yamashita, M.; Torizuka, K.; Sato, T. *Opt. Lett.* **1988**, *13*, 24.
(6) Le Moigne, J.; Hilberer, A.; Kajzar, F. *Makromol. Chem.* **1992**, *192*, 515.
(7) Masuda, T.; Higashimura, T. *Adv. Polym. Sci.* **1987**, *81*, 121.
(8) Beltzung, L.; Strazielle, C. *Makromol. Chem.* **1984**, *185*, 1155.
(9) Kajzar, F.; Messier, J. *Thin Solid Films* **1985**, *132*, 11.
(10) Le Moigne, J.; Hilberer, A.; Strazielle, C. *Polym. Prepr. (Am. Chem. Soc., Div. Polym. Chem.)* **1991**, *32*, 96.
(11) Neher, D.; Keitbeitzel, A.; Wolf, A.; Bubeck, C.; Wegner. *J. Phys. D.: Appl. Phys.* **1991**, *24*, 1193.
(12) Van Beek, J. B.; Kajzar, F.; Albrecht, A. C. *J. Chem. Phys.* **1991**, *95*, 6400.
(13) (a) Shirakawa, H.; Ito, T.; Ikeda, S. *Polym. J.* **1973**, *4*, 460. (b) Kuzmany, H. *Phys. Status Solidi* **1980**, *97B*, 521.
(14) Percec, V.; Rinaldi, P. L. *Polym. Bull.* **1983**, *9*, 548.
(15) Cowie, J. M. G. *Polymers: Chemistry and physics of modern materials*; Blackie: New York, 1991; (a) p 247. (b) *Ibid.*; p 209.
(16) Aime, J. P.; Ramakrishnan, S.; Chance, R. R.; Kim, M. W. *J. Phys. (Paris)* **1990**, *51*, 963.
(17) Rossi, G.; Chance, R. R.; Silbey, R. *J. Chem. Phys.* **1989**, *90*, 7594.
(18) Masuda, T.; Isobe, E.; Higashimura, T. *Macromolecules* **1985**, *18*, 841.
(19) Muramatsu, H.; Ueda, T.; Ito, K. *Macromolecules* **1985**, *18*, 1634.
(20) Furlani, A.; Napoletano, C.; Russo, M. V.; Feast, W. J. *Polym. Bull.* **1986**, *16*, 311.
(21) (a) Percec, V. *Polym. Bull.* **1983**, *10*, 1. (b) Bott, D. C.; Brown, C. S.; Winter, J. N.; Barker, J. *Polymer* **1987**, *28*, 601. (c) This particular point will be developed in a paper in preparation.
(22) Neher, D.; Wolf, A.; Leclerc, M.; Keitbeitzel, A.; Bubeck, C.; Wegner, G. *Synth. Met.* **1990**, *37*, 249.

Registry No. I, 70152-91-9; II, 144003-06-5; III, 137790-61-5; IV, 137790-62-6; TMSA, 1066-54-2; PPAC1, 115859-42-2; PPAC2, 137790-56-8; PPAC4, 137790-58-0; PPAC8, 137790-60-4; PPAPh, 144003-08-7.